Pamukkale Üniversitesi Mühendislik Bilimleri Dergisi
Pamukkale University Journal of Engineering Sciences

The role of welding parameters in enhancing joint strength and durability for AISI 1040 and 316 steels

AISI 1040 ve 316 çeliklerinde birleşim dayanımı ve dayanıklılığın artırılmasında kaynak parametrelerinin rolü

Yalçın YAŞAR[1], İbrahim ASLAN[2], Halil Burak KAYBAL[3], Harun YAKA[4]*

[1]Vocational and Technical Anatolian High School, Metal Technology, Tokat
yalcin_yasar@hotmail.com
[2]Motor Vehicles and Transportation Technologies, Taşova Yüksel Akın Vocational School, Amasya University, Amasya, Türkiye
ibrahim.aslan@amasya.edu.tr
[3]Industrial Design, Faculty of Fine Arts, Kırıkkale University, Kırıkkale, Türkiye.
hburak@kku.edu.tr
[4]Department of Mechanical Engineering, Engineering Faculty, Amasya University, Amasya, Türkiye.
harun.yaka@amasya.edu.tr

Received/Geliş Tarihi: 23.01.2025 Revision/Düzeltme Tarihi: 07.04.2025 doi: 10.5505/pajes.2025.74611
Accepted/Kabul Tarihi: 14.04.2025 Research Article/Araştırma Makalesi

Abstract

This study evaluates the effects of welding parameters, particularly amperage, on the mechanical properties and microstructures of AISI 1040 and AISI 316 steels joined using Electric Arc Welding (EAW), Metal Inert Gas (MIG), and Tungsten Inert Gas (TIG) welding techniques. Experimental samples were subjected to tensile, bending, and microhardness tests, followed by microstructural analysis using optical microscopy. The results showed that welding amperage significantly influences tensile and bending strengths, as well as hardness values. For AISI 1040 steel, TIG welding at 100 amperes achieved the highest tensile strength (543 MPa) and bending strength (181 N), while EAW at 70 amperes exhibited the lowest values. For AISI 316 stainless steel, MIG welding at 70 amperes yielded the highest tensile strength (491 MPa), and EAW at 90 amperes demonstrated the highest bending strength (150 N). Microhardness analysis indicated that rapid cooling in surface regions increased hardness. Microstructural examination revealed grain refinement and uniformity at optimal amperages, contributing to improved mechanical properties. The study underscores the importance of selecting appropriate welding parameters to enhance joint performance and weld quality.

Keywords: Welding parameters; AISI 1040 steel; AISI 316 stainless steel; Mechanical properties; Microstructural analysis

Öz

Bu çalışma, kaynak parametrelerinin, özellikle akım şiddetinin, Electric Arc Welding (EAW), Metal Inert Gas (MIG) ve Tungsten Inert Gas (TIG) kaynak teknikleri ile birleştirilen AISI 1040 ve AISI 316 çeliklerinin mekanik özellikleri ve mikro yapıları üzerindeki etkilerini değerlendirmektedir. Deneysel örnekler, gerilme, eğilme ve mikrosertlik testlerine tabi tutulmuş ve ardından optik mikroskopi ile mikro yapı analizi yapılmıştır. Sonuçlar, kaynak akımının, gerilme ve eğilme dayanımları ile sertlik değerlerini önemli ölçüde etkilediğini göstermiştir. AISI 1040 çeliği için, 100 amperde yapılan TIG kaynağı en yüksek gerilme dayanımını (543 MPa) ve eğilme dayanımını (181 N) sağlarken, 70 amperde yapılan EAW kaynak işlemi en düşük değerlere sahiptir. AISI 316 paslanmaz çelik için ise, 70 amperde yapılan MIG kaynağı en yüksek gerilme dayanımını (491 MPa), 90 amperde yapılan EAW kaynağı ise en yüksek eğilme dayanımını (150 N) göstermiştir. Mikrosertlik analizi, yüzey bölgelerinde hızlı soğumanın sertliği artırdığını belirtmiştir. Mikro yapı incelemesi, optimal akım şiddetlerinde tane incelmesi ve uniformluk sağlandığını, bunun da mekanik özellikleri iyileştirdiğini ortaya koymuştur. Çalışma, uygun kaynak parametrelerinin seçilmesinin, birleşim performansını ve kaynak kalitesini artırmadaki önemini vurgulamaktadır.

Anahtar kelimeler : Kaynak parametreleri; AISI 1040 çeliği; AISI 316 paslanmaz çeliği; Mekanik özellikler; Mikroyapı analizleri

1 Introduction

Welding is a critical fabrication process utilized across various industries, with several methods frequently employed, each offering distinct applications and advantages. Among the most widely used techniques are Electric Arc Welding (EAW), Metal Inert Gas (MIG) welding, and Tungsten Inert Gas (TIG) welding. MIG welding is valued for its speed and versatility, making it suitable for thin materials and automated operations. TIG welding, on the other hand, is renowned for producing high-quality, precise welds, particularly in stainless steel and aluminum applications. Each method necessitates specific techniques and equipment, enabling welders to choose the most appropriate approach based on material properties and project requirements [1-3].[2]

While each welding method has its advantages, they also have disadvantages. Selecting appropriate welding parameters based on the method and material characteristics is essential. The most critical parameter in the welding process is amperage [4]. The amperage determines how much heat the welding process will create on the material and thus how strong a weld bond will be formed. Low amperages are generally used on thin materials, providing a more careful and controlled weld. High amperages are used to make stronger welds on thicker and stronger materials. If the amperage is not adjusted correctly, several negative situations may occur. If low amperages are used, insufficient heat is produced, and the welding line may be

*Corresponding author/Yazışılan Yazar
*Corresponding author/Yazışılan yazar

weak. The material cannot be fully melted, and a good connection cannot be achieved. High amperages can create excessive heat on the material, causing the material to burn or deform [5,6]. Many studies have been carried out to determine the correct welding parameters. Venkatratnam and Rao (2020) examined dissimilar joints of AISI 202 and AISI 316 steels, produced using Metal Inert Gas (MIG) welding. Welding current, wire feed speed, gas flow rate, and edge preparation angle were chosen as production parameters. Tensile strength, impact strength, and maximum bending load were obtained as outputs of the study [7]. Açar et al. (2023) investigated the weldability of dissimilar stainless steels using different gas combinations with MIG welding. AISI 316 austenitic stainless steel and AISI 430 ferritic stainless steel were joined using MIG welding with various shielding gas combinations. The welded sheets underwent metallographic testing as well as hardness, tensile, and bending tests. The effects of these parameters on mechanical and microstructural properties were analyzed [8].

Ogbonna et al. (2023) used the gray-based Taguchi method to optimize multiple responses in TIG welding for AISI 1008 mild steel and AISI 316 stainless steel. The gray-integrated Taguchi optimization approach was applied to optimize welding process parameters-such as current, voltage, and gas flow rate-based on multiple performance characteristics, including ultimate tensile strength, yield strength, elongation percentage, and Vickers microhardness of the weld zone. The study identified welding current as the most critical parameter influencing multiple performance characteristics of the welded joint [9]. Ramakrishnan et al. (2021) conducted experimental research on the mechanical properties of TIG-welded dissimilar AISI 304 and AISI 316 stainless steels using 308 filler rods. But joints were created with three different current levels. The study examined the effects of welding current on TIG welding and employed various mechanical tests to control the mechanical properties of the weld. The current levels were set at 30, 45, and 60 amperes, while the corresponding voltages were 40 V, 60 V, and 80 V. Hardness and tensile tests were performed on each sample [10]. Ongun et al. (2017) studied the effects of heat treatment on the mechanical properties of AISI 1040 steel joined by electric arc and MIG welding. Tensile, three-point bending, notched impact, and hardness tests were conducted on both heat-treated and untreated samples. The tensile deformation of the untreated samples was found to be higher than that of the welded samples [11]. Adin (2024) performed a parametric study on the mechanical properties of dissimilar cylindrical steel joints of AISI 1040 and AISI 8620, welded using MIG and TIG techniques. Additionally, the fracture surfaces of the samples were examined using scanning electron microscopy (SEM) and energy-dispersive X-ray analysis (EDAX) [12]. Sakthivel and Sivakumar (2014) investigated the effects of vibration in TIG and arc welding of AISI 316 stainless steel. Their research revealed that welding with mechanical vibrations resulted in smoother and finer-grained structures [13]. Math and Kumar (2022) qualitatively examined the effects of shielded metal gas welding techniques (MIG and TIG) on AISI 1040 steel. Parameters such as arc voltage, arc current, welding speed, nozzle-to-work distance, and gas pressure were found to significantly influence welding quality. The thickness of the support plate and the material itself also played a crucial role [14]. Ateş et al. (2017) investigated the mechanical and microstructural characteristics of AA5XXX aluminum plates connected by MIG welding. They carried out several tensile, bending, and hardness tests. Compared to the untreated material (UT), tensile strengths of 12 h and 24 h sub-zero temperature treated (CT) specimens increase substantially by 12% and 14%, respectively [15].

Improper selection of amperage in welding processes can result in suboptimal welding quality, diminished joint strength, and potential defects such as porosity, incomplete fusion, or excessive spatter. These issues not only compromise the structural integrity of the weld but also increase the likelihood of premature failure in critical applications. Therefore, determining the optimal amperage values is paramount to ensuring high-quality welds that meet both mechanical and structural performance standards. In this study, extensive experimental investigations were carried out to identify the ideal amperage values for the selected materials and welding methods. By analyzing the influence of amperage on the mechanical properties and microstructural characteristics of the welds, this research aims to provide valuable insights into parameter optimization. The findings are expected to contribute to the development of standardized practices for welding AISI steels, enhancing joint strength and durability across various industrial applications. Furthermore, this work builds upon the existing body of knowledge by addressing the interplay between amperage and other key welding parameters, ultimately paving the way for more efficient and reliable welding processes.

2 Material and methods

In this study, AISI 1040 and AISI 316 materials with dimensions of 3x150x300 mm were used. Each material was joined using Electric Arc, MIG, and TIG welding methods. For Electric Arc Welding of low-carbon steel, 3.25 mm diameter rutile electrodes were used, while for stainless steel, 3.25 mm diameter electrodes containing Cr-Ni were employed. In MIG welding of low-carbon steel, SG3 brand welding wire conforming to EN ISO 636-A W4Si1 standards with a 1 mm diameter was used. For stainless steel, welding wire conforming to EN ISO 14343-A G199 LSI standards with a 0.8 mm diameter was utilized. For TIG welding, low-carbon steel was joined using 1.6 mm diameter Mo70 filler wire, while TW308L wire was employed for stainless steel. The chemical composition of the TW308L wire was 0.45 Si, 1.70 Mn, 20 Cr, 10 Ni, and 0.15 Mo. Argon gas with a purity of 99.99% was used as a shielding gas in MIG and TIG welding. The gas flow rate was set to 10 liters per minute. Tungsten electrodes with a 1.6 mm diameter were utilized.

2.1 Welding parameters

Different current values were used in Electric Arc Welding (EAW). For both low-carbon and stainless steel, three different current levels were applied. The welding parameters for each material are detailed in Tables 1 and 2.

Table 1. Electric arc welding parameters for AISI 1040 steel.

	Amperage	Electrode Diameter (mm)	Duration (s)	Current Type
EAK70	70	3.25	100	DC
EAK80	80	3.25	90	DC
EAK90	90	3.25	85	DC

Table 2. Electric arc welding parameters for AISI 316 stainless steel.

	Amperage	Electrode Diameter (mm)	Duration (s)	Current Type
EAK70	70	3.25	100	DC
EAK80	80	3.25	90	DC
EAK90	90	3.25	87	DC

In MIG welding, different current levels were applied. Tables 3 and 4 present the parameters for low-carbon and stainless steel, respectively.

Table 3. MIG welding parameters for AISI 1040 steel.

	Amperage	Electrode Diameter (mm)	Duration (s)	Current Type
MIG70	70	1.00	98	DC
MIG80	80	1.00	93	DC
MIG90	90	1.00	84	DC

Table 4. MIG welding parameters for AISI 316 stainless steel.

	Amperage	Voltage	Electrode Diameter (mm)	Duration (s)	Current Type
MIG70	70	16	0.8	100	DC
MIG80	80	16.8	0.8	95	DC
MIG90	90	17.2	0.8	87	DC

In TIG welding, three different current levels were applied for both materials. The parameters are presented in Tables 5 and 6.

Table 5. TIG welding parameters for AISI 1040 steel.

	Amperage	Electrode Diameter (mm)	Duration (s)	Current Type
TIG80	80	1.60	245	DC
TIG90	90	1.60	240	DC
TIG100	100	1.60	237	DC

Table 6. TIG welding parameters for AISI 316 stainless steel.

	Amperage	Electrode Diameter (mm)	Duration (s)	Current Type
TIG80	80	2.00	246	DC
TIG90	90	2.00	242	DC
TIG100	100	2.00	236	DC

2.2 Tensile testing

Tensile test samples for the welded steel and stainless steel materials were prepared in accordance with TS 5789 standards using a laser cutting unit. Samples were prepared with the dimensions specified in Figure 1. From each welded plate, three tensile test samples were extracted and tested, and the average values were determined.

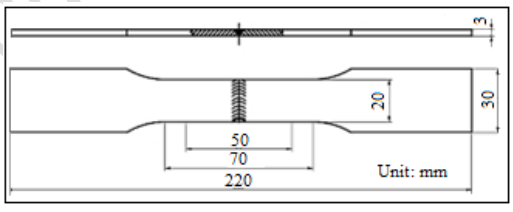

Figure 1. Dimensions of tensile test samples as per TS EN 5789 standards.

Tensile-elongation diagrams were plotted based on the parametric values of the samples. Tensile tests were conducted to evaluate the mechanical properties of the butt-welded materials and assess the influence of welding current on joint properties.

2.3 Bending testing

Samples from each material, welded under specified parameters, were subjected to bending tests using a bending test device. The tests were conducted using the three-point bending method in accordance with ASTM E190-14 standards. The procedure for the bending test is schematically presented in Figure 2.

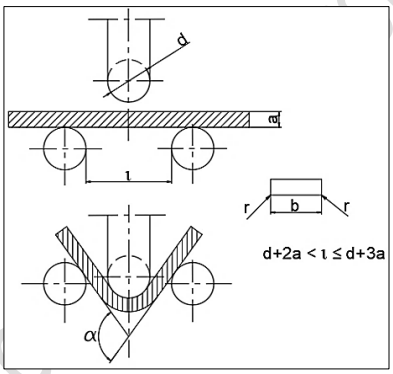

Figure 2. Schematic of bending test sample.

2.4 Microhardness testing

Hardness scans were performed on samples obtained from all welded materials using a Vickers microhardness tester. Measurements were taken starting from the base material, progressing through the HAZ (Heat Affected Zone) and weld metal, at 0.5 mm intervals. The test load was set at 50 g (HV 0.05).

2.5 Macro and microstructure analysis

Samples from the welded materials were mounted in bakelite to facilitate handling. They were sequentially ground with 60, 200, 400, 600, 800, and 1200 grit sandpapers under water, changing the sanding direction at each stage. The polished samples were further refined with alumina powder on a felt cloth. After washing with water, the samples underwent electrolytic etching. The welded surfaces of the prepared samples were examined under a Nikon microscope, as shown in Figure 3.

Figure 3. The image of the Nikon Eclipse L150A optical microscope.

3 Results and discussion

3.1 Tensile test results

The tensile test samples, having been subjected to different welding currents, exhibited varying mechanical properties and elongation values. In the study, AISI 1040 steel joined using EAW (Electric Arc Welding) at 70 amperes for 100 seconds experienced insufficient heat input, leading to inadequate fusion and fracture in the weld zone. At 80 and 90 amperes, fusion improved significantly. Among the samples, the one welded at 80 amperes demonstrated the highest tensile strength. For MIG welding of AISI 1040 steel at 70 amperes for 98 seconds, inadequate heat input led to insufficient fusion and failure in the weld zone. Similar results were observed at 80 amperes. However, at 90 amperes for 84 seconds, fusion was easier, resulting in higher tensile strength. In TIG welding of AISI 1040 steel at 80 amperes for 245 seconds, insufficient heat input caused inadequate fusion and tearing in the weld zone. The sample welded at 90 amperes fractured in the weld zone. However, at 100 amperes for 237 seconds, fusion was achieved more effectively, yielding higher tensile strength. The tensile test results of AISI 1040 steel joined using EAW, MIG, and TIG at different currents are presented in Figure 4. For AISI 316 stainless steel, EAW at 70, 80, and 90 amperes resulted in insufficient heat input, leading to inadequate fusion and weld zone failure. However, samples welded at 80 and 90 amperes exhibited higher tensile strength. In MIG welding, the sample joined at 70 amperes for 100 seconds showed higher tensile strength compared to those joined at higher currents. Despite improved fusion with increasing current, the lower tensile strength in some cases may be attributed to chromium carbide precipitation. Similarly, in TIG welding, the sample joined at 80 amperes for 246 seconds exhibited higher tensile strength compared to those welded at higher currents. Chromium carbide precipitation, resulting from rapid cooling post-welding, could explain the lower tensile strength. To mitigate this, welded materials were cooled in room-temperature water immediately after welding. The tensile test results of AISI 316 stainless steel joined using EAW, MIG, and TIG at different currents are shown in Figure 5.

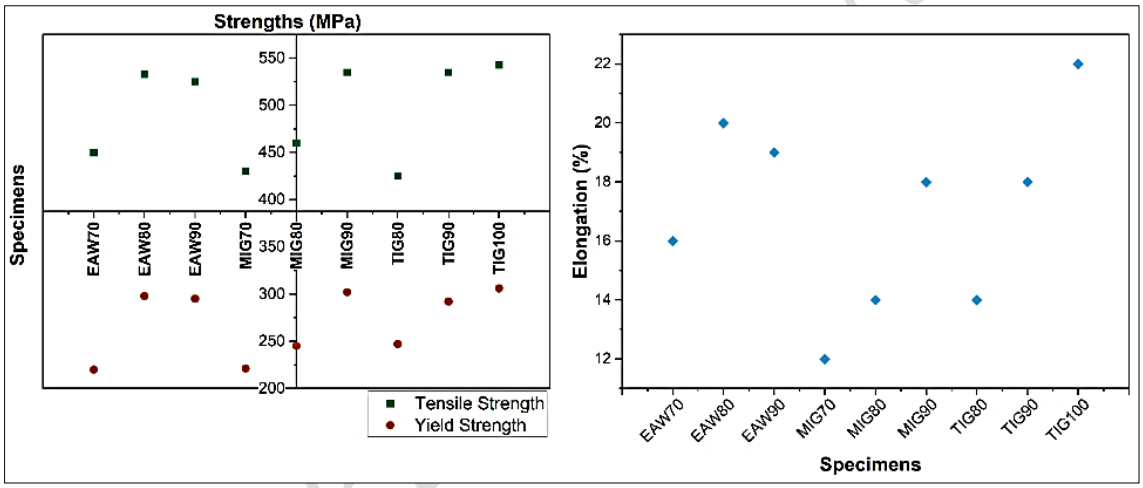

Figure 4. Tensile test results for AISI 1040.

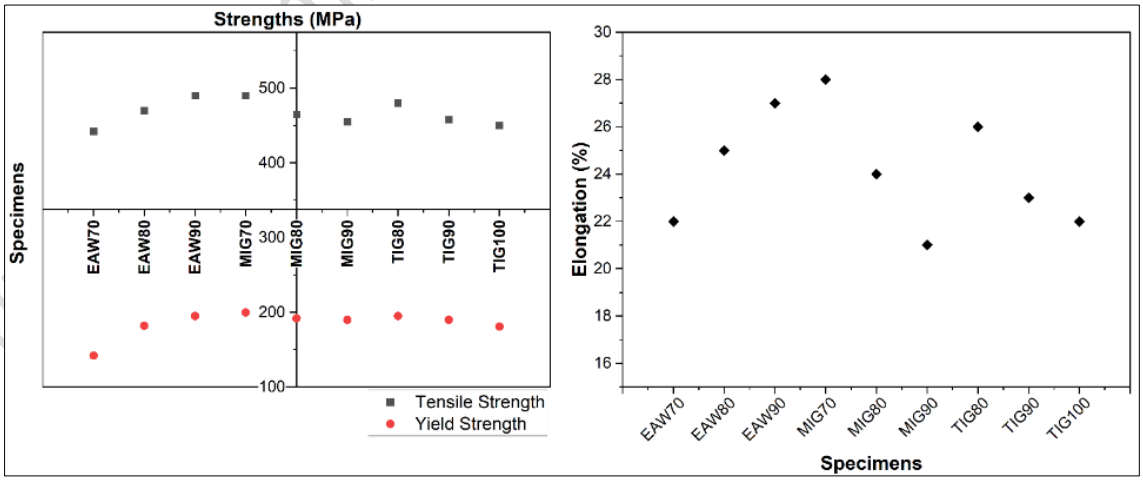

Figure 5. Tensile test results for AISI 316.

3.2 Bending test results

The bending test results for AISI 1040 and AISI 316 stainless steel joined using EAW, MIG, and TIG at three different currents are shown in Figure 6. For AISI 1040 steel, the highest compressive force in EAW and MIG welding was obtained at 80 amperes. In TIG welding, the maximum compressive force was achieved at 100 amperes. The maximum displacement occurred at 90 amperes for EAW and MIG welding, while for TIG welding, it occurred at 100 amperes.

For AISI 316 stainless steel, the highest strength was observed in samples welded at 90 amperes using EAW and TIG. In contrast, for MIG welding, the maximum compressive force was achieved at 80 amperes. The maximum displacement occurred at 90 amperes for EAW and at 80 amperes for MIG and TIG welding.

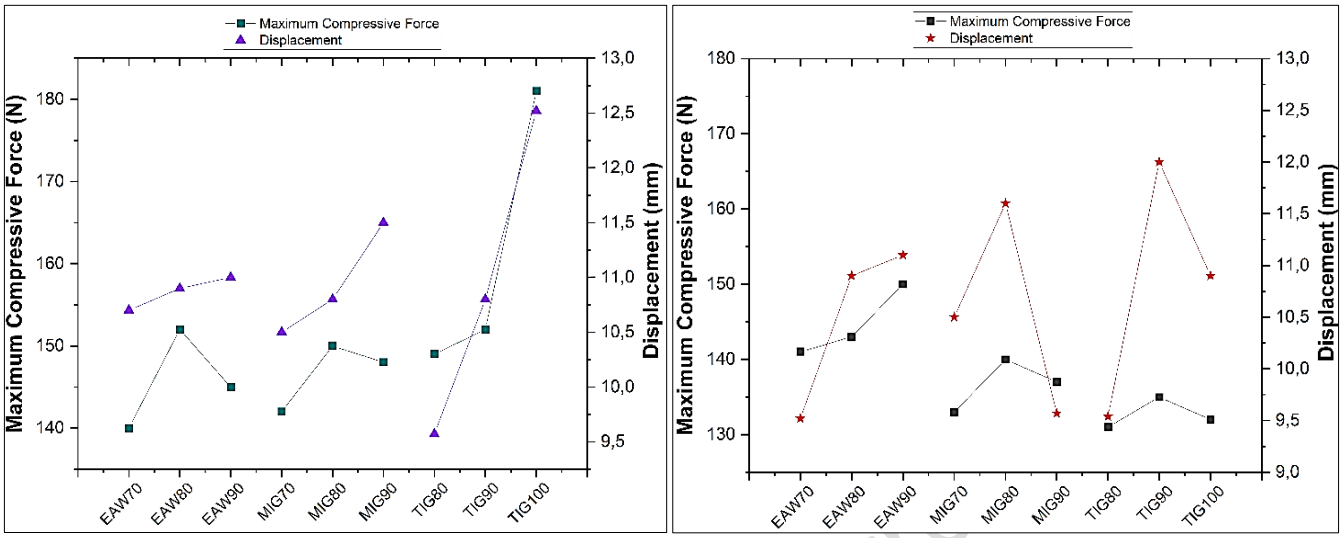

a) b)

Figure 6. Bending test results for a) AISI 1040, b) AISI 316.

3.3 Microhardness test results

Microhardness tests were conducted on samples obtained from all welded parts using a Vickers microhardness tester. Measurements were taken from the base material, HAZ (Heat Affected Zone), and weld metal at 0.5 mm intervals. The test load was set at 50 g (HV 0.05).

The hardness measurement points on the cross-section of the weld zone are shown in Figure 7. The microhardness values for AISI 1040 steel welded using EAW, MIG, and TIG at different currents are presented in Figure 8.

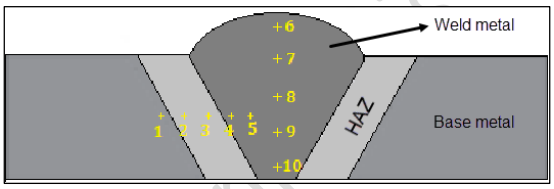

Figure 7. Hardness measurement points.

For EAW, the highest hardness value of 400 kg/mm^2 was observed at point 5 of the sample welded at 80 amperes. In MIG welding, the highest hardness value of 310 kg/mm^2 was observed at point 2 of the sample welded at 80 amperes. In TIG welding, the highest hardness value of 275 kg/mm^2 was recorded at point 6 of the sample welded at 90 amperes. Since point 6 is on the top surface, higher hardness due to rapid cooling is acceptable [16]. The results showed that the base metal had lower hardness values compared to HAZ and weld metal.

The hardness values obtained from welding AISI 316 stainless steel using EAW, MIG, and TIG methods at different current levels are presented in Figure 9. In EAW and MIG welding, the hardest region was found at point 7. Since point 7 is close to the surface, it is normal for it to exhibit relatively higher hardness due to rapid cooling. For EAW, the highest microhardness value of 310 kg/mm^2 was recorded in the sample welded at 90 amperes. In MIG welding, the highest microhardness value was 280 kg/mm^2, also observed in the sample welded at 90 amperes. For TIG welding, the highest hardness value of 245 kg/mm^2 was measured at point 2 of the sample welded at 90 amperes.

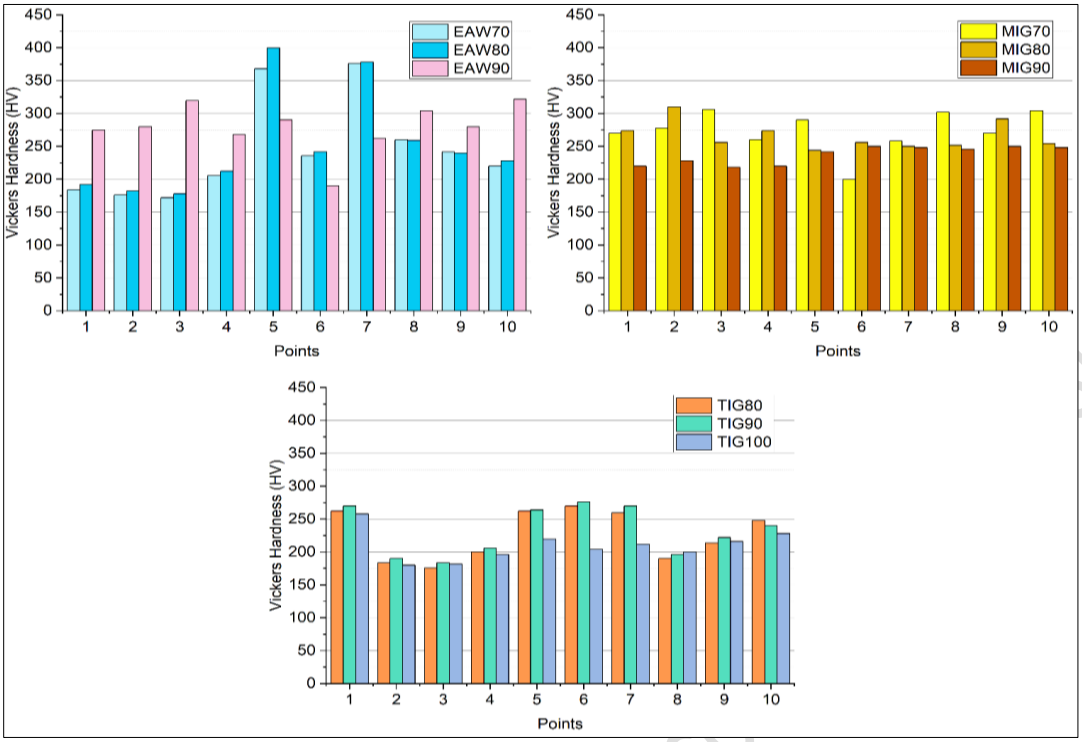

Figure 8. Microhardness values of AISI 1040 steel joined using EAW, MIG, and TIG at different current levels.

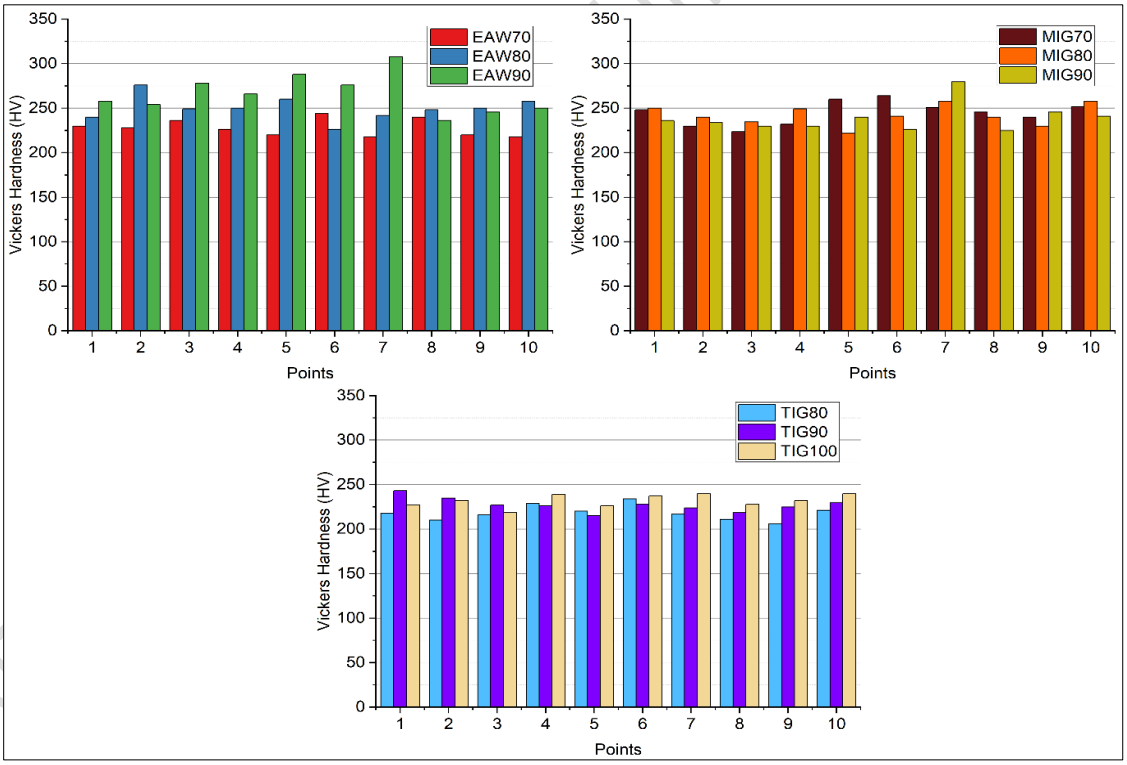

Figure 9. Microhardness values of AISI 316 steel joined using EAW, MIG, and TIG at different current levels.

3.4 Microstructure and macrostructure image analysis

Surface examinations of the weld samples were conducted using a microscope to inspect their microstructures. Images of the samples that exhibited the highest and lowest tensile and compressive strengths for AISI 1040 and AISI 316 steels are provided. The microscopic images of the weld samples are presented in Figures 10, 11, 12, and 13.

For AISI 1040 steel, the lowest tensile strength of 425 MPa was observed in the TIG weld made at 80 amperes, while the highest tensile strength of 543 MPa was achieved in the TIG weld made at 100 amperes. As shown in Figure 10, the grain size of the

sample welded at 100 amperes is smaller and more uniformly distributed compared to the sample welded at 80 amperes. The grain sizes of the base metal and weld metal in the 100-ampere sample are also more consistent. In contrast, grain growth was observed in the weld metal and HAZ of the 80-ampere sample. For AISI 316 stainless steel, the lowest tensile strength of 442 MPa was observed in the EAW weld made at 70 amperes, while the highest tensile strength of 491 MPa was achieved in the MIG weld made at 70 amperes.

As shown in Figure 11, the EAW weld at 70A exhibited two distinct regions within the weld metal. Near the HAZ, a more columnar grain structure was observed, while a more homogeneous grain structure was seen closer to the weld metal. The microstructure of the weld metal was found to consist of austenite and ferrite. In the MIG 70A sample, the weld metal predominantly consisted of austenite. Additionally, differences in grain orientation at the region boundaries created a distinct appearance. This structural alignment contributed to the higher tensile strength of the MIG weld. Uygur (2006) observed fine grains owing to nucleation of martensite and fine precipitates at low welding currents in his study[17].

For AISI 1040 steel, the lowest bending strength of 140 N was observed in the EAW weld made at 70 amperes, while the highest bending strength of 181 N was achieved in the TIG weld made at 100 amperes. As shown in Figure 12, the EAW 70A sample exhibited very small grains in the weld metal, which progressively grew toward the HAZ and base metal. This variation in the microstructure resulted from the heat's influence as it dissipated from the weld point toward the base metal (18). These differences in grain size contributed to the lower bending strength. In the TIG 100A sample, better cooling resulted in finer grains in the weld metal compared to the other samples, leading to the highest bending strength for AISI 1040 steel in the TIG 100A sample. For AISI 316 stainless steel, the lowest bending strength of 131 N was recorded in the TIG weld made at 80 amperes, while the highest bending strength of 150 N was observed in the EAW weld made at 90 amperes. In the TIG 80A sample, the weld metal was predominantly composed of austenite with large grains. In the EAW 90A sample, although austenite was still predominant, the microstructure also included austenite + ferrite. Additionally, the grains in the EAW 90A sample were smaller, which contributed to its higher bending strength.

4 Conclusions

The study comprehensively examined the influence of welding parameters, particularly amperage, on the mechanical properties and microstructures of AISI 1040 and AISI 316 steels joined using Electric Arc Welding (EAW), Metal Inert Gas (MIG), and Tungsten Inert Gas (TIG) welding techniques. The findings demonstrated that for tensile strength, AISI 1040 steel achieved its highest value (543 MPa) with TIG welding at 100 amperes, while the lowest value (425 MPa) was observed with TIG welding at 80 amperes. Similarly, for AISI 316 stainless steel, the highest tensile strength (491 MPa) was attained with MIG welding at 70 amperes, whereas EAW welding at 70 amperes

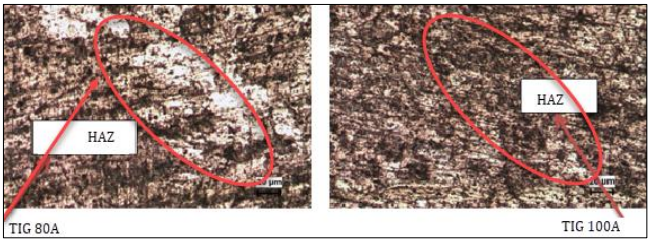

Figure 10. Tensile strength of AISI 1040; lowest in TIG 80A, highest in TIG 100A.

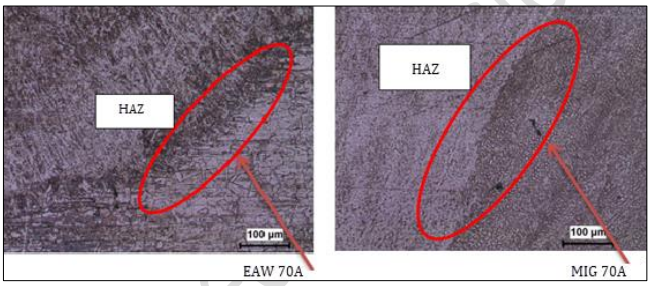

Figure 11. Tensile strength of AISI 316; lowest in EAW 70A, highest in MIG 70A.

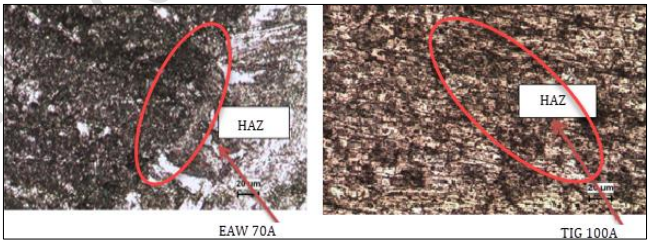

Figure 12. Bending strength of AISI 1040; lowest in EAW 70A, highest in TIG 100A.

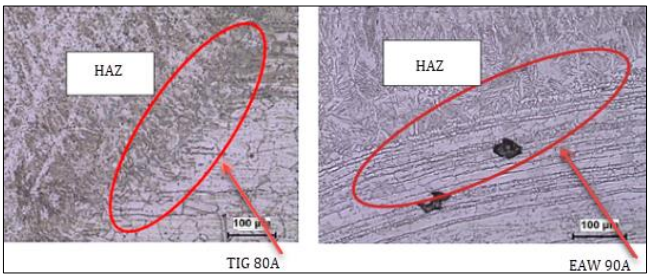

Figure 13. Bending strength of AISI 316; lowest in TIG 80A, highest in EAW 90A.

exhibited the lowest tensile strength (442 MPa). Regarding bending strength, TIG welding at 100 amperes resulted in the highest value (181 N) for AISI 1040 steel, while EAW welding at 70 amperes yielded the lowest (140 N). In AISI 316 stainless steel, the highest bending strength (150 N) was recorded with EAW welding at 90 amperes, and TIG welding at 80 amperes exhibited the lowest (131 N). For microhardness, AISI 1040 steel showed the highest value (400 kg/mm^2) in EAW welding at 80 amperes, while AISI 316 stainless steel achieved its peak microhardness (310 kg/mm^2) with EAW welding at 90 amperes. Microstructural analysis revealed that grain refinement and uniform distribution, particularly in TIG

welding at optimal amperages, contributed to superior mechanical properties, whereas rapid cooling in surface regions caused localized increases in hardness. These results underscore the pivotal role of welding parameters, particularly amperage and cooling conditions, in determining the mechanical and microstructural quality of welded joints, emphasizing the importance of parameter optimization to enhance weld performance.

5 Author contribution statement

Author 1 contributed to the welding processes and experimental procedures. Author 2 was responsible for the literature review. Author 3 evaluated the results, performed the manuscript review, and oversaw the overall supervision of the study. Author 4 contributed to the manuscript writing and its final review. All authors have read and approved the final version of the manuscript.

6 Ethics committee approval and conflict of interest declaration

This study did not involve human participants, animals, or sensitive data requiring ethical approval. Therefore, ethics committee approval was not necessary.

The authors declare that there are no conflicts of interest with any person, organization, or institution regarding the preparation and submission of this manuscript.

7 Nomenclature

EAW Electric arc welding,

MIG Metal inert gas,

TIG Tungsten inert gas,

HAZ Heat-affected zone,

8 References

[1] den Ouden G, Hermans M. *Welding technology*. 1th ed. Delft, Netherlands, VSSD, 2009.

[2] Messler Jr RW. *Principles of welding: processes, physics, chemistry, and metallurgy*. 2nd ed. Singapore, Wiley-VCH, 2008.

[3] Kah P, Latifi H, Suoranta R, Martikainen J, Pirinen M. "Usability of arc types in industrial welding". *International Journal of Mechanical and Materials Engineering*, 9(15), 1-12. 2014.

[4] Apay S. "Optimization of Welding Parameters in MAG Lap Welding of DD13 Sheet Metal with Taguchi Method and FEM Analysis". *Manufacturing Technologies and Applications*, 3(3), 20-30, 2022.

[5] Uygur I, Dogan I. "The effect of TIG welding on microstructure and mechanical properties of a butt-joined-unalloyed titanium". *Metalurgija,* 44(2), 119-123, 2005.

[6] Uygur I, Gulenc B. The Effect of Shielding Gas Compositions for MIG Welding Process on Mechanical Behavior of Low Carbon Steel". *Metalurgija,* 43(1), 35-40, 2004.

[7] Venkatratnam D, Kesava Rao VVS. "Effect of MIG Welding Parameters on Mechanical Properties of Dissimilar Weld Joints of AISI 202 and AISI 316 Steels". *International Journal of Advanced Design and Manufacturing Technology,* 13(2), 51–64, 2020.

[8] Açar I, Çevik B, Gülenç B. "Weldability of dissimilar stainless steels by MIG welding with different gas combinations". *Sādhanā*, 48(2), 69, 2023.

[9] Ogbonna OS, Akinlabi Akinlabi S, Madushele N, Fatoba OS, Akinlabi ET. "Multi-response optimization of TIG dissimilar welding of AISI 1008 mild steel and AISI 316 stainless steel using grey-based Taguchi method". *The International Journal of Advanced Manufacturing Technology*, 126(1–2), 749–758, 2023.

[10] Ramakrishnan A, Rameshkumar T, Rajamurugan G, Sundarraju G, Selvamuthukumaran D. "Experimental investigation on mechanical properties of TIG welded dissimilar AISI 304 and AISI 316 stainless steel using 308 filler rod". *Materials Today: Proceedings*, 45, 8207–8211, 2021.

[11] Ongun A, Uzun İ, Turgut OK. "Investigation of mechanical properties AISI 1040 steel welding with electric arc and MIG, applied various heat treatments". *Pamukkale University Journal of Engineering Sciences*, 23(1), 1–5, 2017.

[12] Adin MŞ. "A parametric study on the mechanical properties of MIG and TIG welded dissimilar steel joints". *Journal of Adhesion Science and Technology*, 38(1), 115–138, 2024.

[13] Sakthivel P, Sivakumar P. "Effect Of Vibration in TIG and Arc Welding Using AISI316 Stainless Steel". *International Journal of Engineering. Research and Science. & Technology*, 3(4), 2014.

[14] Math P, Praveen Kumar BS. "Optimization of Gas Metal Arc Welding Process Parameters on Structural Steel Plates by Taguchi Method". *Journal of Mines, Metals and Fuels,* 70(10A), 254–259, 2022.

[15] Ates H, Tamer Ozdemir A, Uzun M, Uygur I. "Effect of deep sub-zero treatment on mechanical properties of AA5XXX aluminum plates adjoined by MIG welding technique". *Scientia Iranica*, 24(4), 1950-1957, 2017.

[16] Silwal B, Li L, Deceuster A, Griffiths B. "Effect of postweld heat treatment on the toughness of heat-affected zone for grade 91 steel". *Welding Journal,* 92(3), 80-87, 2013.

[17] Uygur I. "Microstructure and wear properties of AISI 1038 H steel weldments". *Industrial Lubrication and Tribology*, 58(6), 303-311, 2006.

[18] Uygur I. "Influence of shoulder diameter on mechanical response and microstructure of FSW welded 1050 Al-alloy". *Archives of Metallurgy and Materials*, 57(1), 53-60, 2012.